Eur J Nucl Med Mol Imaging (2014) 41:946–955
DOI 10.1007/s00259-013-2640-3

ORIGINAL ARTICLE

Association between left ventricular regional sympathetic denervation and mechanical dyssynchrony in phase analysis: a cardiac CZT study

Alessia Gimelli · Riccardo Liga · Dario Genovesi · Assuero Giorgetti · Annette Kusch · Paolo Marzullo

Received: 14 September 2013 / Accepted: 12 November 2013 / Published online: 6 December 2013
© Springer-Verlag Berlin Heidelberg 2013

Abstract
Purpose To evaluate the relationships among myocardial sympathetic innervation, perfusion and mechanical synchronicity assessed with cardiac cadmium-zinc-telluride (CZT) scintigraphy.
Methods A group of 29 patients underwent an evaluation of myocardial perfusion with ^{99m}Tc-tetrofosmin CZT scintigraphy and adrenergic innervation with ^{123}I-metaiodobenzylguanidine (MIBG) CZT scintigraphy. The summed rest score (SRS), motion score (SMS) and thickening score (STS), as well as the summed ^{123}I-MIBG defect score (SS-MIBG), were determined. Regional tracer uptake for both ^{99m}Tc-tetrofosmin and ^{123}I-MIBG was also calculated. Finally, the presence of significant myocardial mechanical dyssynchrony was evaluated in phase analysis on gated CZT images and the region of latest mechanical activation identified.
Results Significant mechanical dyssynchrony was present in 17 patients (59 %) and associated with higher SRS ($P=0.030$), SMS ($P<0.001$), STS ($P=0.003$) and early SS-MIBG ($P=0.037$) as well as greater impairments in left ventricular ejection fraction ($P<0.001$) and end-diastolic volume ($P<0.001$). In multivariate analysis a higher end-diastolic volume remained the only predictor of mechanical dyssynchrony ($P=0.047$). Interestingly, while in the whole population regional myocardial perfusion and adrenergic activity were strongly correlated ($R=0.68$), in patients with mechanical dyssynchrony the region of latest mechanical activation was predicted only by greater impairment in regional ^{123}I-MIBG uptake ($P=0.012$) that overwhelmed the effect of depressed regional perfusion.
Conclusion Left ventricular mechanical dyssynchrony is associated with greater depression in contractile function and greater impairments in regional myocardial perfusion and sympathetic activity. In patients with dyssynchrony, the region of latest mechanical activation is characterized by a significantly altered adrenergic tone.

Keywords ^{123}I-MIBG · CZT · Mechanical dyssynchrony · Phase analysis

Introduction

The assessment of left ventricular (LV) mechanical synchronicity, especially in patients with systolic dysfunction, has gained increasing relevance [1] and phase analysis on gated single photon emission computed tomography (SPECT) has been demonstrated to allow the evaluation of LV mechanical dyssynchrony in an automatic and reproducible manner [2, 3]. While an alteration of myocardial mechanical synchronicity is generally believed to be associated with the presence of overt LV contractile dysfunction, mechanical dyssynchrony has also been reported to occur in patients with normal systolic function [4] associating with an adverse prognosis [5]. Different SPECT-derived functional parameters, i.e. myocardial perfusion abnormalities and impaired myocardial contractile function, have recently been associated with the presence of significant mechanical dyssynchrony in different categories of patients [6, 7]. Likewise, a dysfunction of the cardiac adrenergic nervous system, assessed through ^{123}I-metaiodobenzylguanidine (^{123}I-MIBG) scintigraphy, has consistently been associated with an adverse prognosis [8]. More recently, SPECT technology has

Alessia Gimelli and Riccardo Liga contributed equally to this study.

A. Gimelli (✉) · D. Genovesi · A. Giorgetti · A. Kusch · P. Marzullo
Fondazione Toscana Gabriele Monasterio, Via Moruzzi, 1, 56124 Pisa, Italy
e-mail: gimelli@ftgm.it

R. Liga
Scuola Superiore Sant'Anna, Pisa, Italy

P. Marzullo
CNR, Institute of Clinical Physiology, Pisa, Italy

also been applied to ^{123}I-MIBG imaging, offering the chance to assess cardiac innervation on a regional basis and to compare cardiac sympathetic inhomogeneity with regional myocardial perfusion [9].

An association between dysfunctional cardiac adrenergic innervation, as shown by ^{123}I-MIBG imaging, and myocardial dyssynchrony has been proposed but the evidence is still contradictory, mainly because of the different semiquantitative imaging modalities used, i.e. planar scintigraphy and SPECT, and of the intrinsic regionality of the variable measured [10, 11]. The use of dedicated cardiac cameras with cadmium-zinc-telluride (CZT) detectors, that are characterized by a higher photon sensitivity and spatial resolution [12, 13], might be able to evaluate regional myocardial perfusion, innervation and dyssynchrony with a single-day, low-dose, imaging protocol. Recently, cardiac CZT has been validated against traditional SPECT [4] in the assessment of LV mechanical synchronicity in phase analysis, and has been shown to be able to accurately evaluate regional myocardial contraction despite a limited acquisition time.

We sought to assess, using CZT imaging, the relationships among regional cardiac sympathetic activity, myocardial perfusion and LV mechanical synchronicity in patients with or without LV systolic dysfunction.

Materials and methods

Patient population

The study group comprised 29 consecutive subjects who underwent a combined scintigraphic evaluation of myocardial resting perfusion and adrenergic innervation as part of a study protocol. Specifically, 21 patients with ischaemic heart disease (IHD) and a recent (<1 month) acute myocardial infarction (MI) were evaluated to compare the extent of cardiac adrenergic denervation with the amount of myocardium with compromised perfusion early after revascularization. All patients were treated with primary percutaneous coronary intervention with stenting of the culprit coronary lesion. The mean time to reperfusion from the onset of symptoms was 1.45±0.30 h. In six of ten patients with multivessel disease, ischaemia-causing stenoses on nonculprit coronary vessels were also further treated percutaneously. The characteristics of these patients are summarized in Table 1. Another eight asymptomatic patients, referred for ^{123}I-MIBG scintigraphy because of suspected primary autonomic dysfunction [14], were also studied with ^{99m}Tc-tetrofosmin CZT as part of the study protocol. Exclusion criteria were haemodynamic instability, severely symptomatic heart failure (New York Heart Association, NYHA, class IV), valvular disease of moderate or greater severity, previous percutaneous coronary intervention or by-pass graft surgery, and myocardial infective/inflammatory disease. The presence of symptomatic heart failure (NYHA class ≥2) was recorded. In each patient the presence of left bundle branch block and pathological Q-waves were also determined. Only 4 of 31 patients (13 %) showed left bundle branch block and no patient showed a ventricular paced rhythm. The study was approved by the local Ethics Committee and conformed to the Declaration of Helsinki on human research. Written informed consent was obtained from every patient after they had received an explanation of the protocol, its aims and potential risks.

Table 1 Characteristics of the 21 patients with ischaemic heart disease

Parameter	Value
Demographics and ECG	
Age (years), mean ± SD	64±12
Male gender, *n* (%)	14 (67)
ST-elevated MI, *n* (%)	17 (81)
Pathological Q waves, *n* (%)	16 (76)
Coronary anatomy, *n* (%)	
Single vessel disease	11 (52)
Multi-vessel disease	10 (48)
Culprit coronary artery	
Left anterior descending	16 (76)
Circumflex	0 (0)
Right coronary artery	5 (24)
Localization of MI, *n* (%)	
Anterior segments	15 (71)
Lateral segments	1 (5)
Inferior segments	5 (24)

Acquisition protocol

Each patient underwent a ^{123}I-MIBG CZT scintigraphy scan followed by a planar acquisition using a standard camera and subsequently underwent a ^{99m}Tc-tetrofosmin rest CZT scan using a single-day protocol (74 – 111 MBq for the innervation scan and 185 MBq for the perfusion scan). The mean radiation exposure for the whole protocol was 4.2 mSv (range 3.4 – 5.2 mSv).

^{123}I-MIBG CZT and planar imaging

Patients were pretreated with sodium or potassium perchlorate. Fifteen minutes and 4 h after the intravenous administration of ^{123}I-MIBG dose, a CZT acquisition, lasting 10 min, was performed using a dedicated CZT cardiac camera (Discovery NM 530c; GE Healthcare; Haifa, Israel) equipped with a multiple-pinhole collimator and 19 stationary CZT detectors. Each detector comprised 32×32 pixelated 5-mm thick (2.46×2.46 mm) elements. The system enabled high quality imaging of a three-dimensional volume where the patient's

heart was to be positioned. After CZT acquisition, a 10-min planar image of the anterior thorax was acquired using a dual-headed gamma camera (E.Cam; Siemens Medical Solution; Hoffman Estates, IL), equipped with a low-energy all-purpose parallel-hole collimator. All images were acquired with a 32× 32 matrix and a 20 % energy window centred at the 159 keV photopeak of ^{123}I. Repeat planar and CZT studies were acquired 4 h after injection.

^{99m}Tc-tetrofosmin imaging

After the second MIBG acquisition, rest injection of ^{99m}Tc-tetrofosmin was performed for perfusion evaluation, and from 15 to 30 min after the rest injection, CZT myocardial images were acquired. Acquisitions lasted 8 min and were preceded when indicated by the administration of sublingual nitrates [13]. Patients were imaged in the supine position with arms placed over their head without any detector or collimator motion. All images were acquired with a 32×32 matrix and a 20 % energy window centred at the 140 keV photopeak of ^{99m}Tc.

List mode files were acquired and stored. Images were reconstructed on a standard workstation (Xeleris II; GE Healthcare, Haifa, Israel) using a dedicated iterative algorithm with 50 iterations [12, 13]. A Butterworth postprocessing filter (frequency 0.37, order 7) was applied to the reconstructed slices. The tomographic studies were also reprojected into 60 planar projections to emulate a standard SPECT layout. Images were reconstructed without scatter or attenuation correction.

Qualitative analysis of perfusion and innervation images

^{99m}Tc-tetrofosmin and ^{123}I-MIBG CZT images were semi-quantitatively scored using a 17-segment LV model and a five-point scale (*0* normal, *1* mild, *2* moderate, *3* severe reduction of radioisotope uptake, *4* absence of detectable tracer uptake), as previously described [9]. Visual scoring was performed by two experienced nuclear cardiologists and consensus was reached in the event of discordance. Thus, the summed rest score (SRS) and the summed ^{123}I-MIBG scores (SS-MIBG) were calculated by adding the segmental scores of the perfusion and innervation images, respectively. Finally, from early and delayed planar ^{123}I-MIBG scintigraphic images, the heart-to-mediastinum ratios and the myocardial washout rate were calculated as previously described [15]; no background correction was performed.

Quantitative analysis of perfusion and innervation images

Quantitative analysis was performed using normalized polar maps with the same 17-segment LV model. Segmental radiotracer uptake was calculated for both the ^{99m}Tc-tetrofosmin and ^{123}I-MIBG scans and expressed as percentage of the peak tracer uptake. In addition, a regional evaluation of myocardial perfusion and innervation was performed using commercially available software (Corridor4DM; Invia, Ann Arbor, MI) using a five-region model of LV myocardium. This model separately considered the LV anterior, lateral, inferior and septal wall, and the apex (Figs. 1 and 2). Accordingly, the regional tracer uptake for both the ^{99m}Tc-tetrofosmin and ^{123}I-MIBG scans was calculated. Considering the previously published data on ^{123}I-MIBG distribution in normal subjects [16] showing a similar tracer distribution in early and delayed images and the generally worse image quality of delayed images, only the early ^{123}I-MIBG SPECT dataset was used for further analyses. Indeed, in our population the summed ^{123}I-MIBG scores from the early and delayed ^{123}I-MIBG scans, as a measure of regional tracer uptake, were strongly correlated (Fig. 3). Finally, in the 21 of 29 patients with IHD and recent MI, the walls with a relative ^{99m}Tc-tetrofosmin uptake <50 % were considered necrotic.

Analysis of gated images

LV volumes and ejection fraction were measured from gated ^{99m}Tc-tetrofosmin images using the same software as used previously. LV volumes were further indexed in relation to body surface area. The summed motion score (SMS) and the summed thickening score (STS) were also obtained using the same software package [17, 18]. CZT-derived measures of global and regional myocardial systolic function have recently been validated against magnetic resonance imaging [19].

Evaluation of LV mechanical dyssynchrony

Mechanical dyssynchrony was evaluated using previously described software [21]. Briefly, after the initial automatic localization of endocardial and epicardial boundaries, this software applies a three-dimensional geometrical approach with a hybrid sampling structure to calculate regional cardiac volumes for each frame and to derive the time from end diastole to the minimum value, analogous to the time to peak contraction (TTP). The TTP of a region is defined as the percentage of the cardiac cycle at which the contraction is maximal [20].

The phase analysis is displayed by means of contractility curves, where each myocardial region (anterior, lateral, inferior and septal wall, and the apex) is separately represented, and a contractility histogram, where the phase distribution of all myocardial regions is displayed. The standard deviation (SD) of the phase distribution and the histogram bandwidth, during which 95 % of myocardium initiates contraction, are automatically generated and expressed as percentage of the cardiac cycle. All dyssynchrony measures were further converted into degrees by multiplying by 3.6 (360/100) [22]. The

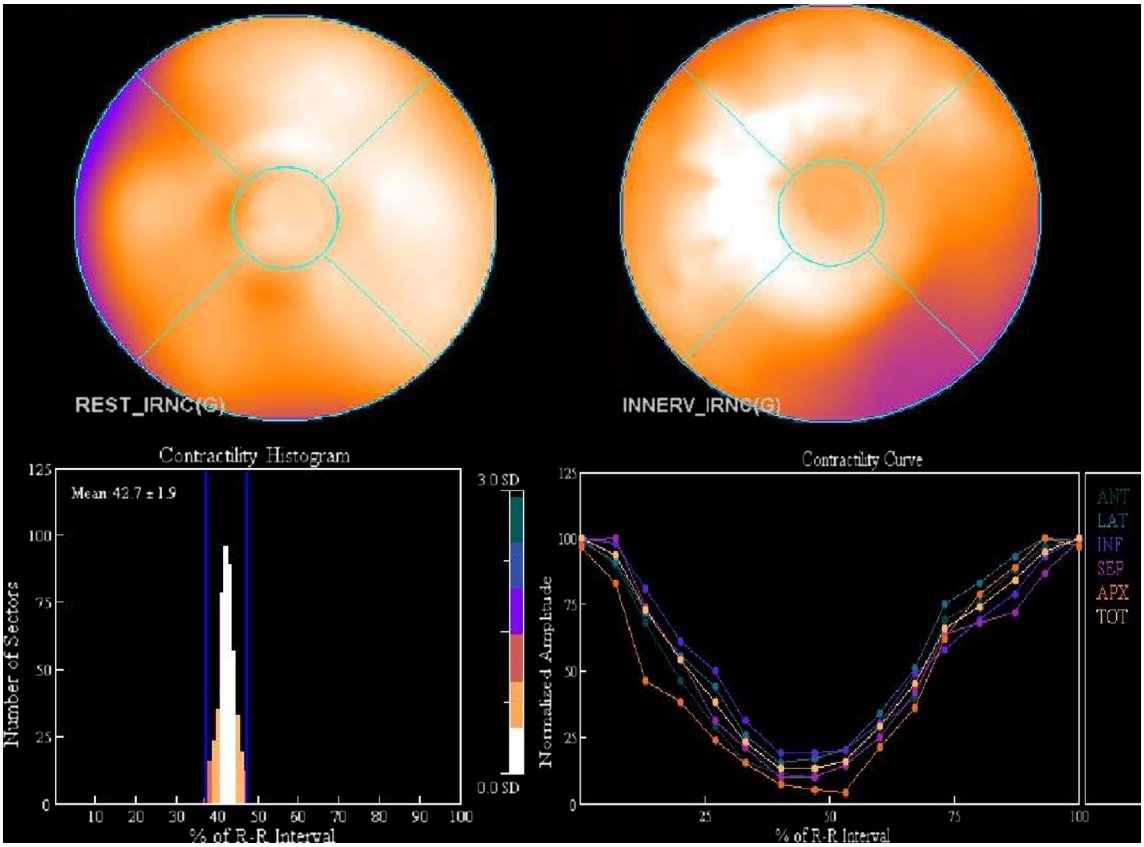

Fig. 1 ^{99m}Tc-tetrofosmin (*upper left*) and early ^{123}I-MIBG (*upper right*) distribution polar plots, contractility histogram (*lower left*) and regional contractility curves (*lower right*) in a patient with normal perfusion, innervation and synchronicity

presence of mechanical dyssynchrony was diagnosed when the phase bandwidth and/or the SD exceeded by two SDs the previously published reference values for healthy men (bandwidth 39±12°; SD 14±5°) and women (bandwidth 31±10°; SD 12±5°) [2]. In this respect, CZT-derived measures of cardiac mechanical synchronicity have recently been shown to be superimposable on those obtained with traditional SPECT cameras [4].

As previously reported [22], in patients with mechanical dyssynchrony, the region of latest mechanical activation of the LV myocardium was automatically identified by the software algorithm using the same five-region LV model of the perfusion study. When the latest contracting region was represented by the apex, the most delayed nearby myocardial wall was also considered in subsequent analyses.

Statistical analysis

Continuous variables are expressed as means ± SD and categorical variables as percentages. Groups were compared using Fisher's exact test for categorical data and analysis of variance for continuous variables followed by Fisher's PLSD for multiple comparisons. All tests were two-sided. Logistic regression models were used to identify the determinants of mechanical dyssynchrony on a per-patient basis and a per-wall basis. Only variables with a P value <0.05 in univariate analyses were included in the multivariate models. The predictive value of a variable was expressed as the odds ratio (OR) with corresponding 95 % confidence interval (CI); the Wald test was used for significance. A P value <0.05 was considered significant.

Statistical analyses were performed using JMP statistical software (SAS Institute Inc, version 4.0.0) and Stata software (Stata Statistical Software, release 10; StataCorp. 2007, College Station, TX).

Results

Characterization of the study population

Patients with a recent MI (75 % of the whole population) showed a higher SRS (18 vs. 6; P=0.002), STS (18 vs. 8; P=0.047) and lower LV ejection fraction (47 vs. 63; P=0.048) than those with suspected primary autonomic dysfunction. However, the dissimilar clinical presentation was not associated

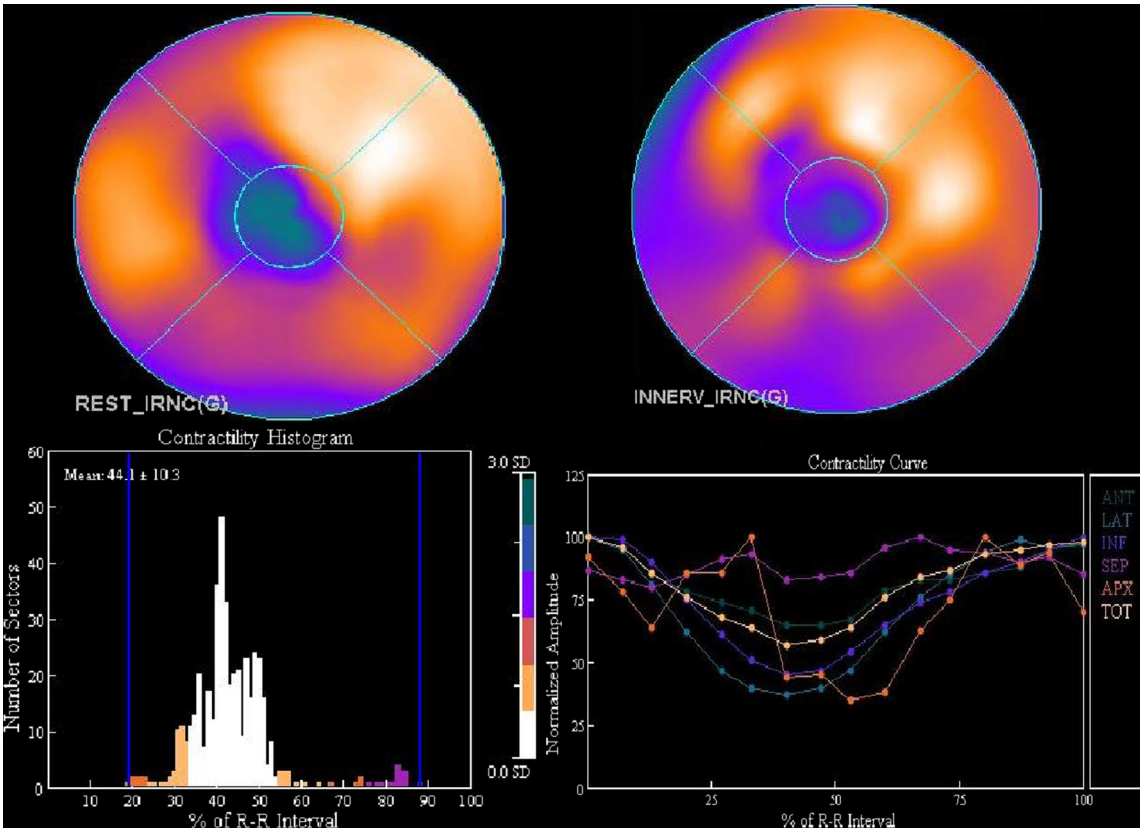

Fig. 2 ^{99m}Tc-tetrofosmin (*upper left*) and early ^{123}I-MIBG (*upper right*) distribution polar plots, contractility histogram (*lower left*) and regional contractility curves (*lower right*) in a patient with recent ST-elevated MI. A large area of innervation/perfusion mismatch encompassing the entire septal wall is apparent. Phase analysis shows significant mechanical dyssynchrony with septal asynergy

with significant differences in demographics, cardiovascular risk factor prevalence, measures of cardiac adrenergic innervation activity (heart-to-mediastinum ratios, myocardial washout rate and SS-MIBG values) and indicators of LV mechanical synchronicity (histogram bandwidth and SD). In the whole population, significant mechanical dyssynchrony in the phase analysis was recognized in 17 of 28 patients (59 %), 14 of whom had suffered a recent MI while 3 had suspected primary autonomic dysfunction ($P=0.218$).

According to the presence of mechanical dyssynchrony, the population was divided into two groups (Tables 2 and 3). Patients with mechanical dyssynchrony were more frequently male ($P=0.010$) than those without dyssynchrony. As shown in Table 2, patients with mechanical dyssynchrony were characterized by significantly higher LV end-diastolic ($P<0.001$) and end-systolic ($P<0.001$) volumes than those without dyssynchrony. Finally, the presence of mechanical dyssynchrony was associated with significantly altered SRS ($P=0.030$), STS ($P=0.003$) and SMS ($P<0.001$), as well as a greater degree of abnormality in early SS-MIBG ($P=0.014$), as an index of regional sympathetic innervation heterogeneity. Conversely, no differences in the indexes of global myocardial adrenergic innervation, heart-to-mediastinum ratio and washout rate, were observed.

Predictors of LV mechanical dyssynchrony: per-patient analysis

The relationships among LV functional parameters, myocardial perfusion and innervation measures on cardiac CZT scintigraphy and mechanical dyssynchrony were further assessed (Table 4). Different variables were associated with mechanical dyssynchrony in the univariate analysis (EDV index, SRS, STS, SMS, early SS-MIBG). Interestingly, in the multivariate analysis, the presence of a higher EDV index ($P=0.047$)

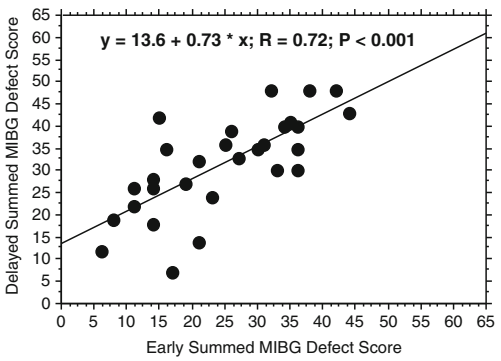

Fig. 3 Relationship between early and delayed summed ^{123}I-MIBG scores

Table 2 Characteristics of the patients

Parameter	Overall population (n=29)	Dyssynchrony present (n=17)	Dyssynchrony absent (n=12)	P value
Demographics and symptoms				
Age (years), mean ± SD	66±12	64±12	69±11	0.340
Male gender, n (%)	16 (55)	13 (76)	3 (25)	0.010
NYHA class ≥2, n (%)	8 (28)	8 (47)	0 (0)	0.009
Left bundle branch block, n (%)	4 (14)	4 (24)	0 (0)	0.121
Cardiovascular risk factors, n (%)				
Family history of CAD	8 (28)	4 (24)	4 (33)	0.683
Diabetes	7 (24)	5 (29)	2 (17)	0.665
Hypercholesterolaemia	24 (83)	14 (82)	10 (71)	0.999
Low HDLc	13 (45)	10 (59)	3 (25)	0.130
Hypertension	22 (76)	13 (76)	9 (75)	0.999
Smoking	11 (38)	8 (47)	3 (25)	0.273
Obesity	8 (28)	6 (35)	2 (17)	0.408

remained the only predictor of significant mechanical dyssynchrony.

Predictors of LV mechanical dyssynchrony: per-wall analysis

The region of latest mechanical activation was located in the inferior, septal and lateral wall in four patients (24 %), four patients (24 %), and two patients (11 %), respectively. In seven patients (41 %) the latest contracting region was located in the apex. In these patients, the most delayed nearby myocardial wall was the septal, lateral and inferior wall in three, two and two patients, respectively. As shown in Fig. 4, both relative myocardial ^{99m}Tc-tetrofosmin and ^{123}I-MIBG uptake gradually reduced in cardiac regions of patients without mechanical dyssynchrony, in normally contracting walls of patients with mechanical dyssynchrony, and in regions with delayed mechanical activation.

The relationships among myocardial perfusion, innervation and regional myocardial dyssynchrony were further investigated. In the overall population (Fig. 5), as well as in patients with (R=0.66, P<0.001) and without (R=0.56, P=0.001) IHD, there was a significant correlation between the quantitative normalized myocardial ^{99m}Tc-tetrofosmin and ^{123}I-MIBG

Table 3 Nuclear imaging data (means ± SD)

Parameter	Overall population (n=29)	Dyssynchrony present (n=17)	Dyssynchrony absent (n=12)	P value
Perfusion and functional data				
Summed rest score	14±10	18±9	10±10	0.030
Summed thickening score	15±12	20±11	8±8	0.003
Summed motion score	17±16	26±14	4±6	<0.001
End-diastolic volume (EDV) index (ml/m^2)	79±39	102±36	47±11	<0.001
End-systolic volume index (ml/m^2)	44±36	65±33	14±6	<0.001
Ejection fraction (%)	52±20	38±12	71±8	<0.001
Myocardial innervation parameters				
Early heart-to-mediastinum ratio	1.52±0.21	1.53±0.20	1.51±0.24	0.878
Delayed heart-to-mediastinum ratio	1.46±0.23	1.44±0.20	1.48±0.28	0.607
Washout rate (%)	30±14	28±12	32±17	0.404
Early summed MIBG defect score	25±11	29±9	18±11	0.014
Delayed summed MIBG defect score	32±11	33±9	29±14	0.362
Dyssynchrony data				
TTP (°)	167±19	174±19	157±13	0.015
Standard deviation of TTP (°)	35±21	48±19	17±4	<0.001
Histogram bandwidth (°)	131±84	179±78	63±20	<0.001

Table 4 Determinants of LV dyssynchrony in the per-patient analysis

Variables	Univariate OR (95 % CI)	*P*	Multivariate OR (95 % CI)	*P*
End-diastolic volume index (ml/m^2)	1.19 (1.04 – 1.35)	0.011	1.17 (1.01 – 1.36)	0.047
End-systolic volume index (ml/m^2)	1.78 (0.83 – 3.82)	0.137	NA	NA
Ischaemic heart disease, 1 – 0	3.75 (0.56 – 25.13)	0.173	NA	NA
Summed rest score	1.10 (1.01 – 1.20)	0.041	NS	NS
Summed thickening score	1.14 (1.03 – 1.25)	0.011	NS	NS
Summed motion score	1.25 (1.04 – 1.49)	0.017	NS	NS
Early summed MIBG defect score	1.11 (1.01 – 1.21)	0.024	NS	NS
Delayed summed MIBG defect score	1.04 (0.96 – 1.11)	0.350	NA	NA
Heart-to-mediastinum ratio	0.40 (0.01 – 11.73)	0.592	NA	NA
Washout rate (%)	0.98 (0.93 – 1.03)	0.393	NA	NA

uptake. However, in the logistic regression analysis, a reduced regional myocardial ^{123}I-MIBG uptake (OR 0.95, 95 % CI 0.92 – 0.99; P=0.012) was the only independent predictor of delayed regional myocardial activation in the phase analysis, overwhelming the effect of depressed myocardial perfusion. Moreover, even after exclusion of the myocardial necrotic walls from the multivariate analysis, the independent association between depressed regional innervation and delayed mechanical activation persisted (OR 0.95, 95 % CI 0.91 – 0.99; P=0.018).

Discussion

In patients with or without LV systolic dysfunction, CZT-derived measures of mechanical synchronicity were associated with alterations in regional myocardial perfusion, contractile function and sympathetic innervation. In patients with mechanical dyssynchrony, the region of the latest mechanical activation was characterized by a significantly impaired adrenergic activity, suggesting a functional relationship between regional sympathetic derangement and myocardial synchronicity.

LV mechanical dyssynchrony: clinical characteristics and prognostic impact

While mechanical dyssynchrony has been extensively studied in patients with heart failure and overt LV systolic dysfunction [1], altered mechanical synchronicity has also been reported in patients with mildly depressed or normal LV systolic function [4, 5, 7]. Specifically, the occurrence of LV mechanical dyssynchrony in phase analysis has been reported in patients with a recent acute coronary syndrome and preserved ejection fraction [23], and predicts adverse ventricular remodelling [24]. Gated SPECT imaging offers the chance to combine evaluation of segmental myocardial perfusion with the assessment of LV regional contractile function [3, 24], allowing an accurate evaluation of the relationship between perfusion heterogeneity and regional myocardial mechanical activity.

In our study, phase analysis was performed with a dedicated CZT cardiac camera. These cameras are characterized by a higher spatial resolution than standard cameras [12, 13], and this may allow better assessment of segmental cardiac perfusion and an accurate evaluation of regional synchronicity [4]. Our results confirm that abnormal LV mechanical synchronicity is frequent even in the absence of electrical dyssynchrony [25], and is associated with a greater degree of depression in

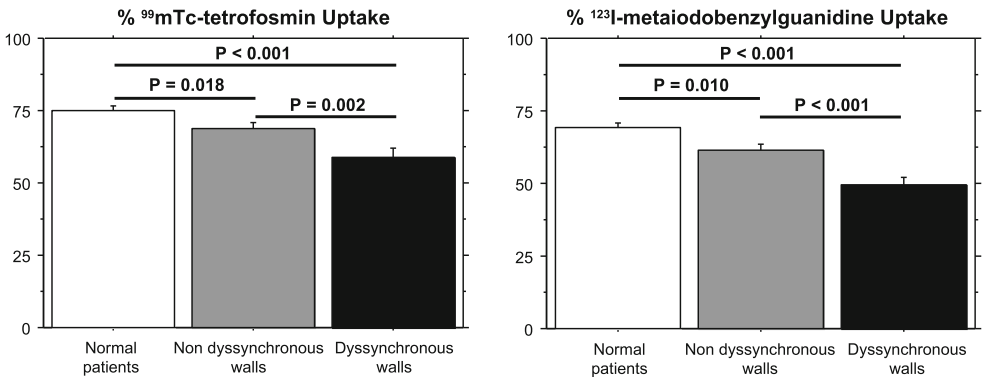

Fig. 4 Normalized regional ^{99m}Tc-tetrofosmin (*left*) and early ^{123}I-metaiodobenzylguanidine (*right*) uptake in cardiac regions of patients without mechanical dyssynchrony, in normally contracting walls of patients with mechanical dyssynchrony (nondyssynchronous walls), and in regions with delayed mechanical activation (dyssynchronous walls)

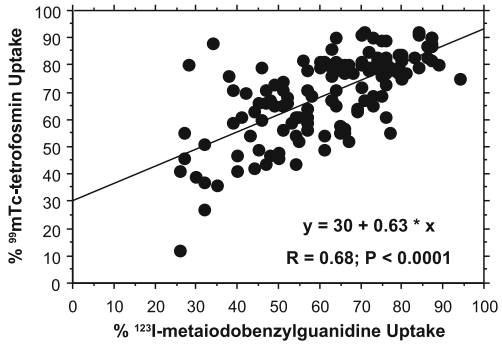

Fig. 5 Relationship between regional normalized early ^{123}I-MIBG and ^{99m}Tc-tetrofosmin uptake. While in the entire population there was a strict correlation between regional myocardial adrenergic activity and perfusion, a small number of regions were characterized by a relatively preserved ^{99m}Tc-tetrofosmin uptake despite a severely depressed sympathetic activity. Since nerve terminals are more susceptible to ischaemic injury, these regions might identify the areas of perinecrotic myocardium that underwent prolonged ischaemia during the acute coronary event

LV systolic function, and greater alterations in measures of myocardial perfusion and regional adrenergic innervation activity. The relationship between LV systolic impairment and mechanical dyssynchrony has already been reported [24]. While higher LV volumes predict the occurrence of LV mechanical dyssynchrony, they are also associated with a significantly lower rate of reverse remodelling after cardiac resynchronization therapy [26]. In our study, LV end-diastolic volume, a measure of cardiac overload, was found to be the strongest predictor of the presence of mechanical dyssynchrony, overwhelming the effect of other functional parameters. Nevertheless, at a regional level, a significant association between delayed mechanical activation, depressed sympathetic innervation and myocardial perfusion was also documented. In patients with mechanical dyssynchrony, delayed myocardial mechanical activation was associated with depressed myocardial perfusion and adrenergic innervation derangement.

Therefore, while our results confirm the general association between impaired LV systolic function and mechanical dyssynchrony, they also demonstrate the association between matched innervation/perfusion impairment and regional myocardial dyssynchronous activation.

Functional predictors of LV mechanical dyssynchrony

The association between abnormal myocardial perfusion, depressed LV systolic function and mechanical synchronicity in phase analysis has been documented [6, 7]. In these studies, conducted mainly in patients with IHD, both the extent of myocardial scarring and the severity of regional and global myocardial contractile impairment predicted the occurrence of LV mechanical dyssynchrony. In patients with a previous MI, an increasing extent of scar tissue is associated with obvious alterations in regional contractility which may profoundly alter overall myocardial synchronicity. Accordingly, in patients with IHD an integrated characterization of regional myocardial perfusion and mechanical synchronicity seems mandatory for evaluating both regional myocardial mechanical activation and the extent of scar tissue.

Our results confirmed that in patients with and without LV systolic dysfunction, myocardial synchronicity is influenced by regional perfusion and contractile function derangement [6, 7], as assessed by gated CZT imaging. However, the present study demonstrated that the presence of abnormal LV mechanical activation is also associated with measures of regional adrenergic derangement, i.e. the early SS-MIBG defect score. Interestingly, the relationship between delayed LV mechanical activation and impaired regional adrenergic tone persisted even after correction for myocardial perfusion and for the presence of myocardial scarring, suggesting an independent association between impaired sympathetic drive and myocardial synchronicity.

Cardiac sympathetic innervation and LV mechanical dyssynchrony

A relationship between altered adrenergic activity and myocardial mechanical dyssynchrony has been suggested, but the results have been contradictory [10, 11]. While measures of cardiac global adrenergic activity derived from planar scintigraphy are widely adopted [9], they might be ineffective in evaluating a phenomenon characterized by intrinsic regionality, such as mechanical dyssynchrony [22, 25].

To our knowledge, this is the first study in which an integrated evaluation of cardiac mechanical synchronicity and regional adrenergic innervation using a CZT camera has been performed, and the study suggested that indexes of regional adrenergic heterogeneity may predict the presence of dyssynchrony better than planar measures. While global measures of cardiac adrenergic innervation have been associated with the presence of mechanical dyssynchrony [11] and with the response to cardiac resynchronization therapy [27], the relationship between regional sympathetic tone and myocardial contractility has been only loosely investigated. Interestingly, in patients with idiopathic LV dysfunction, a significant heterogeneity of regional myocardial perfusion has been reported [15], and its association with mechanical dyssynchrony demonstrated [28]. Likewise, in different categories of patients, a similar heterogeneity of regional sympathetic innervation activity, as evaluated by ^{123}I-MIBG SPECT, has been suggested [10, 15]. Our results confirm the existence of a linear correlation between regional myocardial perfusion and adrenergic innervation [29]. Moreover, the present study demonstrated that in patients with mechanical dyssynchrony the region of the latest mechanical activation is characterized by significantly lower ^{99m}Tc-tetrofosmin and ^{123}I-MIBG uptake. Specifically, while patients with mechanical dyssynchrony showed higher myocardial

perfusion and innervation heterogeneity compared to those with synchronous ventricular activation, a more compromised regional adrenergic activity, as shown by a lower ^{123}I-MIBG uptake, was found to be the only independent predictor of delayed regional myocardial activation, overwhelming the effects of depressed myocardial perfusion and the extent of scarring. Therefore, by demonstrating that a depressed regional myocardial adrenergic tone predicts the presence of LV mechanical dyssynchrony independently of the extent of myocardial perfusion abnormalities, our results suggest a relevant association between regional myocardial contractile function and sympathetic tone. While no pathophysiological conclusions can be drawn from the present study, our data show that measures of regional adrenergic innervation activity might be used in clinical decision-making in patients with mechanical dyssynchrony.

Limitations

The small size of our patient population prevented the assessment of any causal relationship between the variables explored, while the consecutive nature of the enrolment prevented the selection of a homogeneous population of patients, with or without LV dysfunction. Since the study was conducted mainly in patients with IHD, its results should not be extended to different cohorts of subjects. However, as the inclusion of a parallel control population would have been ethically inacceptable, our study was conducted in patients in whom combined evaluation of myocardial perfusion and adrenergic innervation was clinically relevant. Moreover, while measures of delayed ^{123}I-MIBG kinetics are considered more accurate indicators of adrenergic tone, in our study only the early SS-MIBG defect score was associated with the presence mechanical dyssynchrony. Interestingly, an alteration in early ^{123}I-MIBG distribution has already been linked to regional myocardial contractile impairment [29] and depressed early ^{123}I-MIBG uptake is consistently associated with deranged regional myocardial perfusion [15, 29]. Nevertheless, in our study, early SS-MIBG uptake remained the only independent predictor of regional mechanical dyssynchrony even after correction for myocardial perfusion.

Therefore, according to present and previous data, parameters of early ^{123}I-MIBG kinetics might represent integrated measures of both neuronal activity and myocardial perfusion, better predicting myocardial functional impairment than delayed ^{123}I-MIBG distribution parameters [29]. Furthermore, while in normal subjects segmental normalized ^{123}I-MIBG distribution has been shown to be superimposable on early and delayed images [16], in our study the qualitative SS-MIBG defect score was significantly higher in delayed as compared to early scans ($P<0.001$). Since our study mainly included patients with a previous MI, the significantly higher ^{123}I-MIBG washout that takes place at the level of necrotic and perinecrotic myocardial regions [15] might explain the increased SS-MIBG defect score in delayed images as an indirect measure of a higher regional myocardial adrenergic activity heterogeneity.

Another limitation regards the use of beta-blocker therapy. In our population each patient with a recent MI and two of eight patients with suspected primary autonomic dysfunction were on beta-blockers. Beta-blocker therapy has been shown to favourably affect myocardial sympathetic tone by reducing global sympathetic drive and adrenergic innervation heterogeneity [30]. However, considering the short time interval between MI and the CZT scan, with the agreement of the referring physicians, beta-blocker therapy was maintained in each patient.

Moreover, since the myocardial perfusion study was only performed at rest, no scintigraphic evidence of the presence of residual inducible ischaemia can be provided. However, considering the short interval and the absence of any cardiac event between the MI and the CZT study, and that the majority of ischaemia-causing lesions were treated, the effects of inducible myocardial ischaemia on the variables measured can be viewed as negligible. On the other hand, due to the administration of nitrates before the CZT perfusion study in patients with IHD, the SRS can be considered as an accurate measure of residual myocardial viability. Nevertheless, the presence of some transiently hypocontractile, viable, myocardial regions that could regain their function during follow-up cannot be excluded.

Finally, the occurrence of attenuation artefacts cannot be excluded. However, to the best of our knowledge, attenuation correction of scintigraphic images was not performed in any of the previous studies on phase analysis.

Conclusion

Myocardial mechanical dyssynchrony is frequent and is associated with greater alterations in myocardial perfusion, contractile function and adrenergic innervation. In these patients, the region of the latest mechanical activation showed a greater impairment of sympathetic tone, suggesting a relevant association between innervation derangement and myocardial synchronicity.

Conflicts of interest None.

References

1. Heydari B, Jerosch-Herold M, Kwong RY. Imaging for planning of cardiac resynchronization therapy. JACC Cardiovasc Imaging. 2012;5:93–110.

2. Chen J, Garcia EV, Folks RD, Cooke CD, Faber TL, Tauxe EL, et al. Onset of left ventricular mechanical contraction as determined by phase analysis of ECG-gated myocardial perfusion SPECT imaging: development of a diagnostic tool for assessment of cardiac mechanical dyssynchrony. J Nucl Cardiol. 2005;12:687–95.
3. Lin X, Xu H, Zhao X, Folks RD, Garcia EV, Soman P, et al. Repeatability of left ventricular dyssynchrony and function parameters in serial gated myocardial perfusion SPECT studies. J Nucl Cardiol. 2010;17:811–6.
4. Pazhenkottil AP, Buechel RR, Herzog BA, Nkoulou RN, Valenta I, Fehlmann U, et al. Ultrafast assessment of left ventricular dyssynchrony from nuclear myocardial perfusion imaging on a new high-speed gamma camera. Eur J Nucl Med Mol Imaging. 2010;37:2086–92.
5. Aljaroudi W, Aggarwal H, Venkataraman R, Heo J, Iskandrian AE, Hage FG. Impact of left ventricular dyssynchrony by phase analysis on cardiovascular outcomes in patients with end-stage renal disease. J Nucl Cardiol. 2010;17:1058–64.
6. Samad Z, Atchley AE, Trimble MA, Sun JL, Shaw LK, Pagnanelli R, et al. Prevalence and predictors of mechanical dyssynchrony as defined by phase analysis in patients with left ventricular dysfunction undergoing gated SPECT myocardial perfusion imaging. J Nucl Cardiol. 2011;18:24–30.
7. Uebleis C, Hoyer X, Van Kriekinge SD, Schuessler F, Laubender RP, Becker A, et al. Association between left ventricular mechanical dyssynchrony with myocardial perfusion and functional parameters in patients with left bundle branch block. J Nucl Cardiol. 2013;20:253–61.
8. Jacobson AF, Senior R, Cerqueira MD, Wong ND, Thomas GS, Lopez VA, et al. Myocardial iodine-123 meta-iodobenzylguanidine imaging and cardiac events in heart failure. Results of the prospective ADMIRE-HF (AdreView Myocardial Imaging for Risk Evaluation in Heart Failure) study. J Am Coll Cardiol. 2010;55:2212–21.
9. Boogers MJ, Borleffs CJW, Henneman MM, van Bommel RJ, van Ramshorst J, Boersma E, et al. Cardiac sympathetic denervation assessed with 123-iodine metaiodobenzylguanidine imaging predicts ventricular arrhythmias in implantable cardioverter-defibrillator patients. J Am Coll Cardiol. 2010;55:2769–77.
10. Sacre JW, Franjic B, Jellis CL, Jellis CL, Jenkins C, Coombes JS, et al. Association of cardiac autonomic neuropathy with subclinical myocardial dysfunction in type 2 diabetes. JACC Cardiovasc Imaging. 2010;3:1207–15.
11. Tanaka H, Tatsumi K, Fujiwara S, Tsuji T, Kaneko A, Ryo K, et al. Effect of left ventricular dyssynchrony on cardiac sympathetic activity in heart failure patients with wide QRS duration. Circ J. 2012;76:382–9.
12. Herzog BA, Buechel RR, Katz R, Brueckner M, Husmann L, Burger IA, et al. Nuclear myocardial perfusion imaging with a cadmium-zinc-telluride detector technique: optimized protocol for scan time reduction. J Nucl Med. 2010;51:46–51.
13. Gimelli A, Bottai M, Giorgetti A, Genovesi D, Kusch A, Ripoli A, et al. Comparison between ultrafast and standard single-photon emission CT in patients with coronary artery disease: a pilot study. Circ Cardiovasc Imaging. 2011;4:51–8.
14. Kochiadakis G, Marketou M, Koukouraki S, Parthenakis F, Chlouverakis G, Karkavitsas N, et al. Cardiac autonomic disturbances in patients with vasovagal syndrome: comparison between iodine-123-metaiodobenzylguanidine myocardial scintigraphy and heart rate variability. Europace. 2012;14:1352–8.
15. Marini C, Giorgetti A, Gimelli A, Kusch A, Sereni N, L'abbate A, et al. Extension of myocardial necrosis differently affects MIBG retention in heart failure caused by ischaemic heart disease or by dilated cardiomyopathy. Eur J Nucl Med Mol Imaging. 2005;32:682–8.
16. Morozumi T, Kusuoka H, Fukuchi K, Tani A, Uehara T, Matsuda S, et al. Myocardial iodine-123-metaiodobenzylguanidine images and autonomic nerve activity in normal subjects. J Nucl Med. 1997;38:49–52.
17. Lin GS, Hines HH, Grant G, Taylor K, Ryals C. Automated quantification of myocardial ischemia and wall motion defects by use of cardiac SPECT polar mapping and 4-dimensional surface rendering. J Nucl Med Technol. 2006;34:3–17.
18. Sharir T, Berman DS, Waechter PB, Areeda J, Kavanagh PB, Gerlach J, et al. Quantitative analysis of regional motion and thickening by gated myocardial perfusion SPECT: normal heterogeneity and criteria for abnormality. J Nucl Med. 2001;42:1630–8.
19. Giorgetti A, Masci PG, Marras G, Rustamova YK, Gimelli A, Genovesi D, et al. Gated SPECT evaluation of left ventricular function using a CZT camera and a fast low-dose clinical protocol: comparison to cardiac magnetic resonance imaging. Eur J Nucl Med Mol Imaging. 2013;40:1869–75.
20. van der Veen BJ, Al Younis I, Ajmone-Marsan N, Westenberg JJ, Bax JJ, Stokkel MP, et al. Ventricular dyssynchrony assessed by gated myocardial perfusion SPECT using a geometrical approach: a feasibility study. Eur J Nucl Med Mol Imaging. 2012;39:421–9.
21. AlJaroudi W, Jaber WA, Grimm RA, Marwick T, Cerqueira MD. Alternative methods for the assessment of mechanical dyssynchrony using phase analysis of gated single photon emission computed tomography myocardial perfusion imaging. Int J Cardiovasc Imaging. 2012;28:1385–94.
22. Boogers MJ, Chen J, van Bommel RJ, Borleffs CJ, Dibbets-Schneider P, van der Hiel B, et al. Optimal left ventricular lead position assessed with phase analysis on gated myocardial perfusion SPECT. Eur J Nucl Med Mol Imaging. 2011;38:230–8.
23. Lee AP, Zhang Q, Yip G, Fang F, Liang YJ, Xie JM, et al. LV mechanical dyssynchrony in heart failure with preserved ejection fraction complicating acute coronary syndrome. JACC Cardiovasc Imaging. 2011;4:348–57.
24. Murrow J, Esteves F, Galt J, Chen J, Garcia E, Lin J, et al. Characterization of mechanical dyssynchrony measured by gated single photon emission computed tomography phase analysis after acute ST-elevation myocardial infarction. J Nucl Cardiol. 2011;18:912–9.
25. van Bommel RJ, Ypenburg C, Mollema SA, Borleffs CJ, Delgado V, Bertini M, et al. Site of latest activation in patients eligible for cardiac resynchronization therapy: patterns of dyssynchrony among different QRS configurations and impact of heart failure etiology. Am Heart J. 2011;161:1060–6.
26. Tanaka H, Tanabe M, Simon MA, Starling RC, Markham D, Thohan V, et al. Left ventricular mechanical dyssynchrony in acute onset cardiomyopathy: association of its resolution with improvements in ventricular function. JACC Cardiovasc Imaging. 2011;4:445–56.
27. Cha YM, Chareonthaitawee P, Dong YX, Kemp BJ, Oh JK, Miyazaki C, et al. Cardiac sympathetic reserve and response to cardiac resynchronization therapy. Circ Heart Fail. 2011;4:339–44.
28. Brandão SCS, Nishioka SAD, Giorgi MCP, Chen J, Abe R, Martinelli Filho M, et al. Cardiac resynchronization therapy evaluated by myocardial scintigraphy with 99mTc-MIBI: changes in left ventricular uptake, dyssynchrony, and function. Eur J Nucl Med Mol Imaging. 2009;36:986–96.
29. Zhao C, Shuke N, Yamamoto W, Okizaki A, Sato J, Ishikawa Y, et al. Comparison of cardiac sympathetic nervous function with left ventricular function and perfusion in cardiomyopathies by 123IMIBG SPECT and 99mTc-tetrofosmin electrocardiographically gated SPECT. J Nucl Med. 2001;42:1017–24.
30. Chizzola PR, Gonçalves de Freitas HF, Marinho NV, Mansur JA, Meneghetti JC, et al. The effect of beta-adrenergic receptor antagonism in cardiac sympathetic neuronal remodeling in patients with heart failure. Int J Cardiol. 2006;106:29–34.